

## Article

# Characteristics and Impacts of Water–Thermal Variation on Grain Yield in the Henan Province, China, on Multiple Time Scales

Xuefang Feng <sup>1,2</sup>, Feng Wu <sup>2,3,\*</sup>, Songmei Zai <sup>1,2,\*</sup>, Donglin Wang <sup>1,2</sup>, Yuzhong Zhang <sup>1,2</sup> and Qihui Chai <sup>3</sup>

<sup>1</sup> College of Water Conservancy, North China University of Water Resources and Electric Power, Zhengzhou 450046, China

<sup>2</sup> Henan Key Laboratory of Water-Saving Agriculture, Zhengzhou 450046, China

<sup>3</sup> College of Water Resources, North China University of Water Resources and Electric Power, Zhengzhou 450046, China

\* Correspondence: wufeng@ncwu.edu.cn (F.W.); zaisongmei@ncwu.edu.cn (S.Z.)

**Abstract:** Water and thermal resources are changing significantly because of climate change, further affecting important crops, such as grains, worldwide. Previous studies on climate change trends and their impacts on grain yield were mainly conducted on a single time scale, with few studies conducted on multiple time scales. Therefore, here, climate data and grain yield statistics from 1978–2021 in the Henan Province were used to assess how water and thermal changes impact grain yield on multiple time scales. Water and thermal variation were analyzed using the least squares method, Mann-Kendall method, and wavelet analysis method, and grain yield impacts were analyzed using gray correlation method. Results showed increasing trends for  $\geq 0$  °C and  $\geq 10$  °C accumulated temperature and precipitation, with decreased precipitation in spring. The lowest daily minimum temperature increase was 2–3 times the highest daily maximum temperature. Additionally, grain yield fluctuations were caused by climate change. Climate change affected grain yield on all time scales, fluctuating more in autumn than in summer, which was mainly due to changes in temperature followed by precipitation and extreme precipitation. This study provides a scientific basis for the maintenance of food security under climate change.

**Keywords:** climate change; time scale; grain yield; water and thermal resources; 24 solar terms



**Citation:** Feng, X.; Wu, F.; Zai, S.; Wang, D.; Zhang, Y.; Chai, Q. Characteristics and Impacts of Water–Thermal Variation on Grain Yield in the Henan Province, China, on Multiple Time Scales. *Agronomy* **2023**, *13*, 429. <https://doi.org/10.3390/agronomy13020429>

Academic Editor: Weijian Zhang

Received: 26 November 2022

Revised: 5 January 2023

Accepted: 29 January 2023

Published: 31 January 2023



**Copyright:** © 2023 by the authors. Licensee MDPI, Basel, Switzerland. This article is an open access article distributed under the terms and conditions of the Creative Commons Attribution (CC BY) license (<https://creativecommons.org/licenses/by/4.0/>).

## 1. Introduction

The Sixth Assessment Report by the Intergovernmental Panel on Climate Change (IPCC) states that the global average temperature increased by approximately 1.0 °C from 1850–1900 and 1.09 °C from 2011–2020, and predicts that the global average temperature will rise by 1.5 °C during the 2021–2040 period [1]. With the intensification of global warming trend, the instability of the climate system and the frequency and intensity of extreme climate events have increased, harming many natural systems [2–5]. Agriculture is particularly sensitive to climate change, and water and thermal resources are the two most important climate elements that affect the agricultural system [6]. However, changes in water and thermal resources during crop growth and development under different climatic conditions have a massive impact on crop quality and yield, crop irrigation scheduling, and the layout of agricultural production systems, threatening global food security [7–9]. According to The State of Food Security and Nutrition in the World 2021, which was produced by the Food and Agriculture Organization of the United Nations (FAO), an increase in moderate or severe global food insecurity has been observed since 2014, with nearly 12% of the global population facing severe food insecurity in 2020 due to factors such as conflict, climate change, extreme climate events, economic slowdowns and recessions [10]. Hence, it is vital that the variation characteristics of water and thermal

resources and their effects on food production are studied to ensure food security under climate change.

Several researchers have investigated the variation characteristics of water and thermal resources over the crop growing period on the seasonal or annual scale [11–15]. Yu et al. [16] investigated the trend in the date at which the four seasons begin in China using a phenological method to divide the seasons, and found that spring and summer are starting earlier throughout the country, whereas autumn and winter are beginning later. The results also indicated an increasing trend for summer and winter temperatures in the northern regions. Huang et al. [17] examined seasonal temperature and precipitation trends in the Yellow River basin from 1979–2019, with results revealing a significant warming trend in all seasons and varying trends in seasonal precipitation. Based on the CMIP5 model, Lin et al. [18] investigated the variation trends of climate droughts in the Huaihe River Basin and concluded that aridity is likely to increase in the future. Dong et al. [19] explored the variation characteristics of winter temperature (December–February) across the entire Ningxia region based on data from 1961–2013, with results showing an overall increase in the winter temperature and a significant decrease in the  $<0$  °C accumulated temperature. In general, thermal resources in China show an increasing trend on an annual scale; however, the magnitude of this increase is inconsistent between different regions [20,21], and spatial and temporal differences in precipitation include an increasing trend on the southeast coast and in the northwest, and a decreasing trend in the northeast, north, central, and southwest [22].

Numerous studies have investigated the effects of climate change on crop growth and grain yield. For example, climate warming has been found to expand crop cultivation boundaries at higher latitudes and altitudes, prolonging the potential growth periods of crops [23–25]. However, the associated accelerated crop growth ultimately results in reduced biomass and dry matter accumulation with lower quality grain and reduced yield [26]. Based on the trend analysis and Mann-Kendall analysis methods, Zhao et al. [27] analyzed the grain yield response to climate change in the Guanzhong region of the Shaanxi Province and found an increasing trend in yield from 1983–2016, indicating that climate yield is positively correlated with temperature. Influenced by both temperature and precipitation, the potential climatic productivity of maize in the Henan Province has shown an inverted U-shaped dynamic change over time [28]. Zhang et al. [29] explored the sensitivity of grain yields to climate change using a nonlinear regression model, with results indicating that wheat and summer maize yields in the Henan Province were most sensitive to average temperature and total sunshine hours during the reproductive season. Pang et al. [30] comprehensively assessed the annual variation in agricultural climate resources (light, temperature, and water) during the rice growing season in the southwest region and found that precipitation is the main factor affecting the potential climatic productivity of single-season rice. In a study by Yang et al. [31], the relationship between grain yield and cultivated land in Tibet was analyzed to identify the main factors affecting grain yield. The results suggested that the most important factors are cultivated area,  $\geq 0$  °C accumulated temperature, and precipitation during the growing season. Zai et al. [32] pointed out that crops do not fully use climate resources when their productivity is based on annual climate elements, and suggested that the research time scale should be shortened.

The above studies explored climate change trends and their effects on grain yield in different regions; however, there are still some shortcomings. First, most studies have used physical periods or months to distinguish the seasons, with few studies based on the 24 solar terms. The 24 solar terms have a guiding value for agricultural farming activities, mainly because they reflect climate changes in temperature, precipitation, and season, which still have a guiding effect on agricultural farming. Second, these studies have been conducted on a single time scale, with fewer studies conducted on multiple time scales. The Henan Province is not only one of the major grain-producing regions in China but is also the birthplace of the 24 solar terms [33,34]. Hence, it is essential that the trend of climate

change in Henan Province and its effect on grain yield is analyzed based on multiple time scales.

In this study, ground observation data and grain yield statistics data from 1978–2021 for Zhengzhou City, Henan Province, were analyzed, and  $\geq 0$  °C accumulated temperature,  $\geq 10$  °C accumulated temperature, precipitation and extreme climate were selected as indicators. The main objectives of this study were to: (1) analyze the variation trends and cycles in water and thermal resources at annual and seasonal scales, (2) analyze the variation characteristics of grain yield and climate yield, and (3) discuss the correlations between climate indicators and grain yield in Zhengzhou City, Henan Province. Our study provides a scientific basis upon which water and thermal resources can be utilized, ensuring food security in Henan Province under climate change.

## 2. Data and Methods

### 2.1. Study Area

The Henan Province ranges from 31°23' to 36°22' N latitude, 110°21' to 116°39' E longitude, and borders Anhui Province and Shandong Province in the east, Hebei Province and Shanxi Province in the north, Shaanxi Province in the west, and Hubei Province in the south, covering a total area of 16,700 km<sup>2</sup>. The Henan Province also includes approximately 0.815 million hectares of crop planting area and produces approximately 10% of the total grain yield in China, rendering it a major grain-producing region. The province is characterized by a continental monsoon climate with four distinct seasons in terms of rain and heat, with wheat and maize comprising the main grain crops. Zhengzhou was selected as the study area, as it represents the climate change characteristics over the entire province (Figure 1).

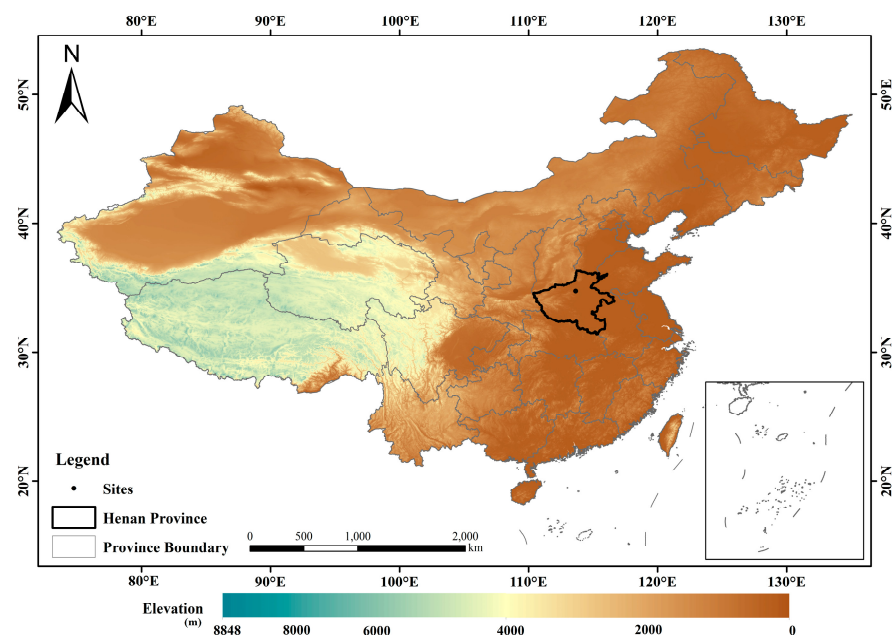


**Figure 1.** Map of the study area. Colors represents the elevation and dot represents the study site at Zhengzhou City in Henan Province.

### 2.2. Data

In this study, the meteorological data are the daily mean temperature, daily maximum temperature, daily minimum temperature, and daily precipitation of Zhengzhou city (site 57083, 113°65' E, 34°72' N, altitude 110.4 m) from 1978–2021, which were obtained from the China Meteorological Data Network (<https://www.data.cma.cn/>, accessed on 3 July 2022). Linear interpolation methods were used to fill in any missing measurements. Grain yield data from 1978–2021, summer grain yield and autumn grain yield from 2000–

2021 were obtained from the Henan Statistical Yearbook [35] and the Henan Provincial People's Government (<https://www.henan.gov.cn/2021/12-11/2363731.html>, accessed on 9 August 2022).

### 2.3. Methods

#### 2.3.1. Indicators Used for Water and Thermal Elements

(1) Accumulated temperature. The accumulated temperature is the sum of the daily average temperatures above the biological lower-limit temperature over a certain period [36] and is calculated using:

$$A = \sum_{i=1}^n T_i (T_i \geq B, \text{ when } T_i < B, T_i = 0) \quad (1)$$

where  $A$  represents the accumulated temperature ( $^{\circ}\text{C}$ );  $T_i$  is the daily mean temperature on the  $i$ th day in the period ( $^{\circ}\text{C}$ );  $B$  is the biological lowest limit temperature ( $^{\circ}\text{C}$ );  $n$  is the total number of days in the studied period ( $d$ ).

The  $\geq 0^{\circ}\text{C}$  and  $\geq 10^{\circ}\text{C}$  accumulated temperatures are important indicators for measuring the thermal resources in a region. The biological lowest limit temperature is  $0^{\circ}\text{C}$  for winter wheat and  $10^{\circ}\text{C}$  for summer maize [37,38]. The farming style in the Henan Province is mainly based on the winter wheat–summer maize shifting mode; therefore, the  $\geq 0^{\circ}\text{C}$  and  $\geq 10^{\circ}\text{C}$  accumulated temperatures were calculated on different time scales. Solar terms indicating the beginning of spring, summer, autumn, and winter were used to divide the seasons.

(2) Daily temperature range. Daily temperature range is an important factor that influences crop growth and refers to the difference between the minimum and maximum temperatures on a specific day, reflecting the magnitude of the temperature change on that day.

(3) Extreme temperature and extreme precipitation. The extreme temperature indicates the highest daily maximum temperature and of the lowest daily minimum temperature in a specific period. The extreme precipitation indicator represents the maximum daily precipitation during a period.

#### 2.3.2. Calculation of Changing Water and Thermal Trends

The least squares method was used to analyze the variation trends using the equation:

$$y = b + ax \quad (2)$$

where  $y$  is a climate indicator;  $x$  is the corresponding year;  $a$  and  $b$  are the regression coefficients; and the change rate of the climate indicators is  $10 \times a$ . Significance analysis of the fitted regression equation was performed using a  $t$ -test with a test level of 0.05.

The Mann-Kendall method [39] was used to determine sudden change points in the variables, as follows:

(1) First, the order column  $S_k$  that corresponds to time series  $X_i$  is calculated with  $n$  samples in the sequential case.

$$S_k = \sum_{i=1}^k a_i (k = 1, 2, 3, \dots, i) \quad (3)$$

$$a_i = \begin{cases} 1 & (x_i > x_j, j = 1, 2, 3, \dots, i) \\ 0 & (x_i \leq x_j, j = 1, 2, 3, \dots, i) \end{cases} \quad (4)$$

(2) The average value and variance of  $S_k$  is then determined:

$$E(S_k) = \frac{k(k-1)}{4} \quad (5)$$

$$\text{Var}(S_k) = \frac{k(k-1)(2k+5)}{72} \quad (6)$$

(3) The  $UF_k$  statistics are calculated as:

$$UF_k = \frac{S_k - E(S_k)}{\sqrt{\text{Var}(S_k)}} \quad (7)$$

(4) Finally, the time series  $X_i$  of  $n$  samples is inverted into  $x_n, x_{n-1}, \dots, x_1$ , to obtain the inverse order series of  $S_k$  and  $UB_k$ .

$$UB_k = -UF_k (k = n, n-1, n-2, \dots, 1) \quad (8)$$

The generated  $UF$  and  $UB$  curves and the critical value at a given significance level (significance level of 0.05, critical value  $U_{0.05} = \pm 1.96$ ) are then plotted; the indicators are considered to have undergone sudden change when  $UF$  line crosses the critical value line that begins at the intersection of the  $UF$  and  $UB$  lines.

### 2.3.3. Wavelet Analysis

Wavelet analysis can reveal the variation characteristics of a time series and was therefore used to determine the change cycles in the generated time series [40]. Molet wavelet analysis is useful for describing non-smooth signals and was therefore selected to analyze the change cycles in each time series.

For a given wavelet function  $\psi(t)$ , the continuous wavelet in time series  $f(t) \in L^2(\mathbb{R})$  is transformed as follow:

$$W_f(a, b) = |a|^{-\frac{1}{2}} \int_{-\infty}^{+\infty} f(t) \bar{\psi}\left(\frac{t-b}{a}\right) dt \quad (9)$$

where  $a$  is the scale parameter that reflects the period length of the wavelet;  $b$  is the paralleling parameter that reflects paralleling over time;  $\bar{\psi}(t)$  is the complex conjugate function of  $\psi(t)$ ; and  $W_f(a, b)$  is the wavelet transform coefficient. Since time series are often discrete in practice, the discrete form of the above equation was used:

$$W_f(a, b) = |a|^{-\frac{1}{2}} \Delta t \sum_{k=1}^N f(k\Delta t) \bar{\psi}\left(\frac{k\Delta t - b}{a}\right) \quad (10)$$

The graph of the wavelet transform coefficient is a two-dimensional contour graph for  $W_f(a, b)$ , with  $b$  taken as the horizontal axis and  $a$  as the vertical axis. The variation characteristics in the time series were obtained from the wavelet transform coefficient graph.

Wavelet variance is obtained by integrating the square of the wavelet transform coefficients of  $a$  in the time domain and was calculated using:

$$\text{Var}(a) = \int_{-\infty}^{+\infty} |W_f(a, b)|^2 db \quad (11)$$

### 2.3.4. Climate Yield

The grain yield is composed of two parts: trend yield and climatic yield. Trend yield represents the yield obtained by economic development and increased productivity, whereas climate yield represents the yield obtained due to changes in climatic factors [41]. The climate yield is obtained by removing the trend yields from the actual grain yield.

$$c_t = y_t - g_t \quad (12)$$

where  $t$  is the sample volume;  $c_t$  is the climate yield ( $\text{kg}/\text{hm}^2$ );  $y_t$  is the grain yield ( $\text{kg}/\text{hm}^2$ ); and  $g_t$  is the yield trend ( $\text{kg}/\text{hm}^2$ ).

The HP filtering method [42] is used to obtain the trend yield solving the minimization problem.

$$\min(M) = \min \left\{ \sum_{t=1}^n (y_t - g_t)^2 + \lambda \sum_{t=3}^n [(g_t - g_{t-1}) - (g_{t-1} - g_{t-2})]^2 \right\} \tag{13}$$

Finding the first-order derivative of  $g_1, g_2, \dots, g_n$  for  $M$  and assuming a value of 0 for the derivative generates the equation:

$$\begin{aligned} c_1 &= \lambda(g_3 - 2g_2 + g_1) \\ c_2 &= \lambda(g_4 - 4g_3 + 5g_2 - 2g_1) \\ &\dots \\ c_n &= \lambda(g_n - 2g_{n-1} + g_{n-2}) \end{aligned} \tag{14}$$

Equation (14) can be converted to produce Equations (15) and (16).

$$g = (\lambda F + I)^{-1}y \tag{15}$$

$$F = \begin{bmatrix} 1 & -2 & 1 & 0 & \dots & \dots & \dots & 0 \\ -2 & 5 & -4 & 1 & 0 & \dots & & 0 \\ 1 & -4 & 6 & -4 & 1 & 0 & & 0 \\ \dots & & & & & & & \\ 0 & & & 0 & 1 & -4 & 6 & 4 & 0 \\ 0 & & & & 0 & 1 & -4 & 5 & 2 \\ 0 & \dots & \dots & & & 0 & 1 & -2 & 1 \end{bmatrix} \tag{16}$$

$\lambda$  is obtained from the time scale of the time series and was taken as 100 for annual, 1600 for seasonal, and 14,400 for monthly time series [43].

### 2.3.5. Gray Correlation Analysis

The Gray correlation analysis is used to measure the degree to which specific factors are correlated. Mathematical and statistical methods are limited by the number of samples and the regularity of sample distribution, while Gray correlation analysis is not affected by such limitations [44]. Gray correlation analysis is therefore used to calculate the correlation degree between the reference series and the comparison series, where the grain or climate yields are represented by reference series  $X_0$  and  $\geq 0^\circ\text{C}$  accumulated temperature,  $\geq 10^\circ\text{C}$  accumulated temperature, precipitation, daily temperature range, and extreme precipitation represent the comparison series  $X_i$ . The specific calculation steps are as follows:

(1) The initial value of each time series is first calculated.

$$X'_i = \frac{X_i}{x_i(1)} = (x'_i(1), x'_i(2), \dots, x'_i(k)), i = 0, 1, 2, \dots, m; k = 1, 2, \dots, n \tag{17}$$

(2) The absolute value sequence of the difference between the initial value of the  $X_0$  and  $X_i$  is generated.

$$\Delta_i(k) = |x'_0(k) - x'_i(k)|, i = 1, 2, \dots, m \tag{18}$$

(3) The maximum and minimum values of the absolute value sequence are produced.

$$M = \max_i \max_k \Delta_i(k) \tag{19}$$

$$N = \min_i \min_k \Delta_i(k) \tag{20}$$

(4) The correlation coefficient is calculated.

$$\gamma_{0i}(k) = \frac{N + \xi M}{\Delta_i(k) + \xi M}, i = 1, 2, \dots, m \tag{21}$$

where  $\zeta$  is the resolution coefficient, normally taken as 0.5.

(5) The degree of correlation between  $X_0$  and  $X_i$  is found as:

$$\gamma_{0i} = \frac{1}{n} \sum_{k=1}^n \gamma_{0i}(k) \quad (22)$$

where  $\gamma_{0i}$  denotes the degree of correlation between  $X_0$  and  $X_i$ . The value of  $\gamma_{0i}$  is closer to 1 in this study, indicating significant correlation between  $X_0$  and  $X_i$ .

### 3. Results

#### 3.1. Variation Characteristics of the Accumulated Temperature from 1978–2021

##### 3.1.1. Variation Trends

The variation trends in the accumulated temperature from 1978–2021 are presented in Table 1. The temporal variation trends for  $\geq 0$  °C accumulated temperature and  $\geq 10$  °C accumulated temperature was consistent on different time scales, with increasing trend observed in both (at 0.05 significance). The increase was greater in magnitude for  $\geq 10$  °C accumulated temperature as compared to  $\geq 0$  °C accumulated temperature (except for winter). Under an annual scale, the variation rates are 215.70 °C/10 a and 221.75 °C/10 a for  $\geq 0$  °C accumulated temperature and  $\geq 10$  °C accumulated temperature, respectively, both show significant increasing trends. However, the increasing trend of  $\geq 0$  °C accumulated temperature was only significant in spring, summer, autumn, whereas that of  $\geq 10$  °C was significant in summer, autumn, and winter on the seasonal scale, with results showing 75.16 °C/10 a, 54.88 °C/10 a, 49.92 °C/10 a and 35.74 °C/10 a for  $\geq 0$  °C accumulated temperature in spring, summer, autumn, and winter and 85.91 °C/10 a, 54.97 °C/10 a, 57.85 °C/10 a and 23.01 °C/10 a for  $\geq 10$  °C accumulated temperature, respectively.

**Table 1.** The variation trends and significance of water and thermal elements in Henan Province from 1978–2021 under different time scales. The \* represents passing the 0.05 significance test.

Time Scale	$\geq 0$ °C Accumulated Temperature (°C/a)	$\geq 10$ °C Accumulated Temperature (°C/a)	Precipitation (mm/a)
Spring	7.516 *	8.591	−0.345
Summer	5.488 *	5.497 *	2.043 *
Autumn	4.992 *	5.785 *	1.199
Winter	3.574	2.301 *	0.306
Year	21.570 *	22.175 *	3.202

On an annual scale, the UF statistic was positive and passes the 0.05 significance level after 1995, whereas the intersection of the UF and UB was outside the confidence interval (Figure 2i,j). This indicates that the warming trend in Henan Province only became significant after 1995. However, no significant sudden change characteristics were observed in either the  $\geq 0$  °C accumulated temperature or  $\geq 10$  °C accumulated temperature on an annual scale. The position of the intersection between UF and UB, which was within the confidence interval on the seasonal scale, indicates that a sudden significant change occurred in both  $\geq 0$  °C accumulated temperature and  $\geq 10$  °C accumulated temperature (except summer) on a seasonal basis (Figure 2a–h). In addition, a sudden increase was observed in both  $\geq 0$  °C accumulated temperature and  $\geq 10$  °C accumulated temperature, mainly between the mid to late 1990s to the beginning of the 21st century.

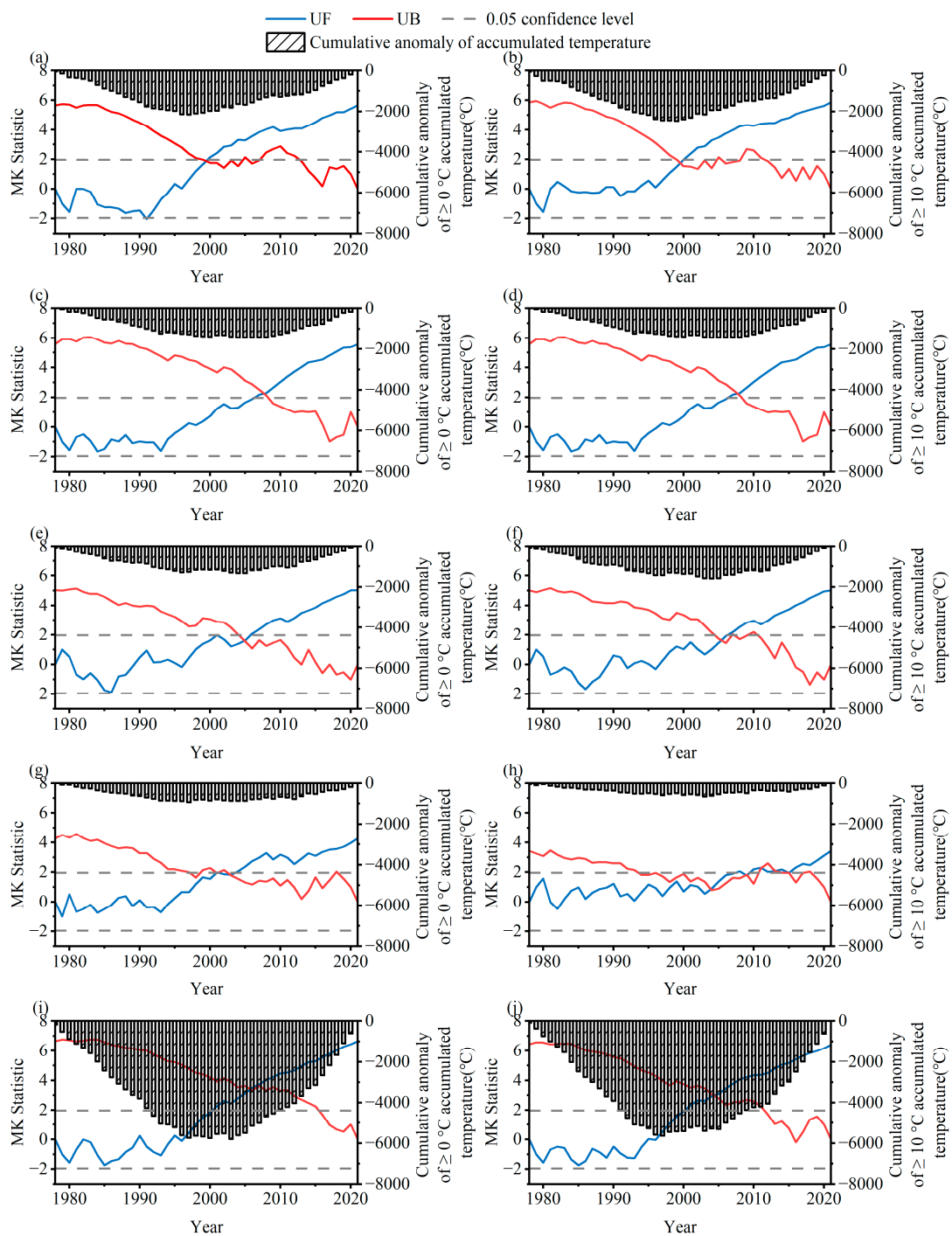


**Figure 2.** The sudden change characteristics of accumulated temperature in Henan Province from 1978–2021 under different time scales. (a–h) represent the seasonal scale, where (a,b) represent spring, (c,d) represent summer, (e,f) represent autumn, and (g,h) represent winter. (i,j) represent the annual scale.

### 3.1.2. Variation Cycles

The variation in the  $\geq 0$  °C accumulated temperature and  $\geq 10$  °C accumulated temperature was consistent, with both presenting alternating positive and negative centers in cycles of approximately 25–30 a throughout the study period (Figure 3a,b). Two low centers and three high centers were observed for  $\geq 0$  °C accumulated temperature and  $\geq 10$  °C accumulated temperature from 1978–2021, with low centers in 1990 and 2008 and high centers in 1982, 2000 and 2016 (Figure 3). Furthermore, no closed center was observed

after 2016 (Figure 3). These results indicate that the  $\geq 0$  °C and  $\geq 10$  °C accumulated temperatures will continue to increase in the future in Henan Province. Additionally, the seasonal variation cycles for  $\geq 0$  °C and  $\geq 10$  °C accumulated temperatures show the same regularity as the annual cycles. Therefore, the seasonal wavelet transform coefficient graph has not been included in this study.

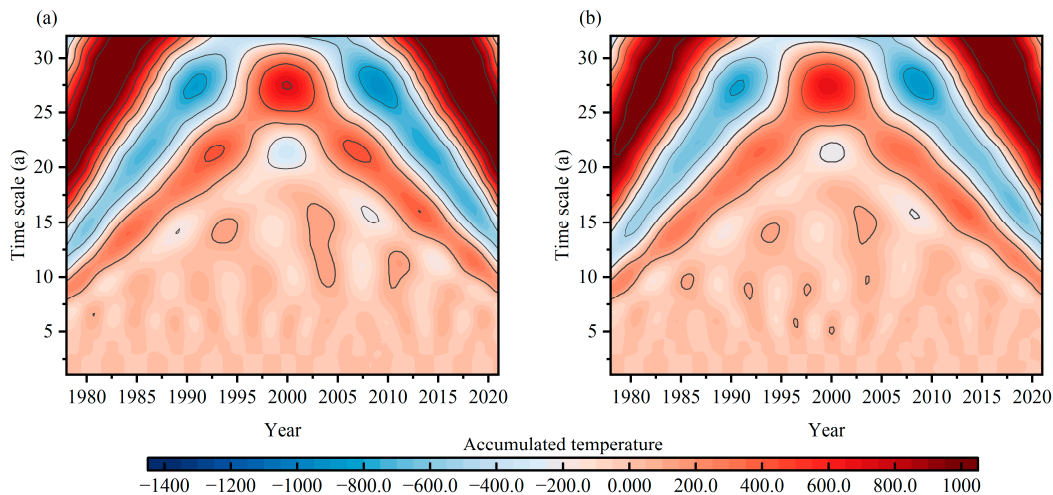


**Figure 3.** The wavelet transform coefficient graph of accumulated temperature in Henan Province from 1978–2021 at the annual scale. (a) represent  $\geq 0$  °C accumulated temperature, and (b) represent  $\geq 10$  °C accumulated temperature.

The main water and thermal cycles in the Henan Province were obtained on different time scales for 1978–2021 using wavelet variance, as shown in Table 2. The first main cycle in  $\geq 0$  °C and  $\geq 10$  °C accumulated temperatures lasted 28 a on both annual and seasonal scales; however, the second main cycle for  $\geq 0$  °C and  $\geq 10$  °C accumulated temperatures of 10 a and 11 a, respectively, occurred only in spring. The results suggest that the variation in  $\geq 0$  °C and  $\geq 10$  °C accumulated temperatures in the Henan Province is likely to decrease over 28 a, along with a short variation cycle of around 10 a in spring.

### 3.2. Variation Characteristics of Precipitation from 1978–2021

#### 3.2.1. Variation Trends

A non-significant increasing trend in precipitation was observed from 1978–2021 on the annual scale, with a variation rate of 32.02 mm/10 a (Table 1). However, a decreasing trend that was observed for precipitation in spring on the seasonal scale was non-significant, while the increasing trend in summer was significant (passing the 0.05 significance test), and non-significant in autumn and winter. Variation rates of  $-3.45$  mm/10 a, 20.43 mm/10 a, 11.99 mm/10 a and 3.06 mm/10 a were observed for spring, summer, autumn and winter, respectively (Table 1). Overall, the climate in the Henan Province is expected to be “warmer and wetter” in the future, both on an annual scale and in the summer, autumn, and winter on a seasonal scale; however, the region is expected to become “warmer and drier” in spring.

The UF statistic was positive in 1978–1980, 1982–1987, and after 2003 on the annual scale; however, this was within the confidence interval (i.e., it did not pass the 0.05 significance level), which indicated the increasing trend in precipitation observed for the Henan Province during the study period was insignificant (Figure 4e). On a seasonal scale, the UF statistic was positive in summer after 1998, passing the 0.05 significance level (Figure 4b). A significantly increasing trend in summer precipitation was observed after 1998. Similarly, a non-significantly increasing trend in spring precipitation was observed during the 1978–1980 and 1989–2004 periods (Figure 4a), with a non-significantly increasing trend in autumn precipitation in 1978–1989 and after 2010 (Figure 4c) and a non-significantly increasing

trend in winter precipitation after 1988 (Figure 4d). Several UF and UB intersections were within confidence intervals. Sudden change in precipitation occurred on an annual scale in 1979, 1983, 1998, 2006, 2009, and 2020. However, more sudden changes were observed on a seasonal scale.

**Table 2.** The main cycles of water and thermal elements in Henan Province from 1978–2021 under different time scales.

Treatments	Time Scale	The First Main Cycle (a)	The Second Main Cycle (a)	The Third Main Cycle (a)
$\geq 0\text{ }^{\circ}\text{C}$ accumulated temperature	Spring	28	10	
	Summer	28		
	Autumn	28		
	Winter	28		
	Year	28		
$\geq 10\text{ }^{\circ}\text{C}$ accumulated temperature	Spring	28	11	
	Summer	28		
	Autumn	28		
	Winter	28		
	Year	28		
Precipitation	Spring	8	21	13
	Summer	18	30	9
	Autumn	29	15	6
	Winter	22	6	8
	Year	27	18	8

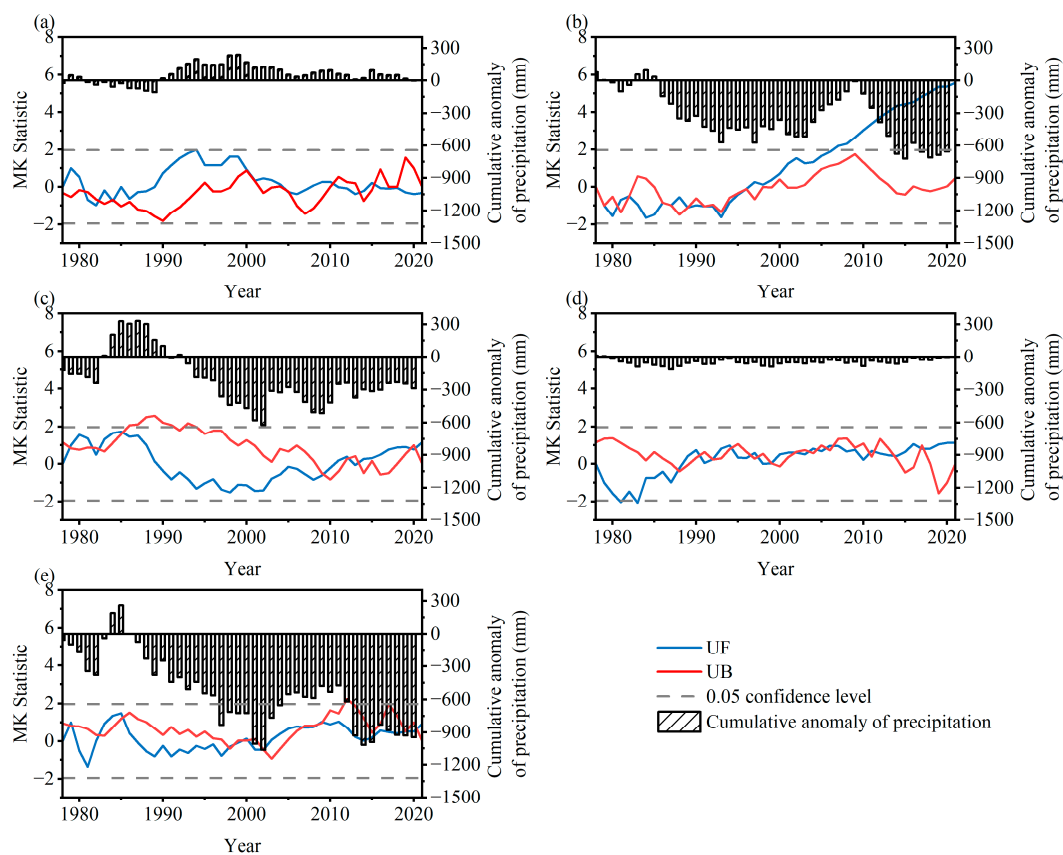


**Figure 4.** Variation characteristics of precipitation in Henan Province from 1978–2021 under different time scales. (a–d) represent the seasonal scale, where (a) represents spring, (b) represents summer, (c) represents autumn, and (d) represents winter. (e) represents the annual scale.

### 3.2.2. Variation Cycles

Three variation precipitation cycles of approximately 23–28, 15–20, and 7–10 years were observed throughout the study period on the annual scale, (Figure 5). Precipitation reached three low and two high centers during the study period, with lows in 1980, 1995 and 2015, and highs in 1988 and 2005. Precipitation is expected to continue to increase after 2021 (Figure 5). Three main cycles were also observed on the annual scale 27, 18, and 8 years. The main cycle on the annual scale differed to that on the seasonal scale, with similarity observed only in the main precipitation cycle during autumn (Table 2).

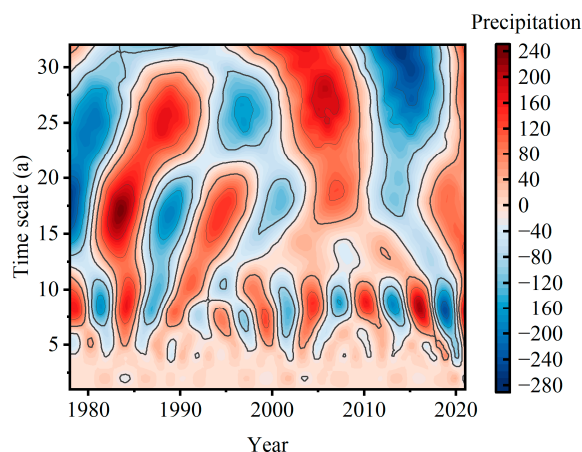


**Figure 5.** The wavelet transform coefficient graph of precipitation in Henan Province from 1978–2021 at the annual scale.

### 3.3. Variation Characteristics of the Extreme Temperature and Precipitation from 1978–2021

The variation trends for extreme temperature and precipitation in the Henan Province from 1978–2021 at different time scales are presented in Table 3. A significant increasing trend was observed in extreme temperature on all time scales, except the highest daily maximum temperature in winter. We also found that the increase in the lowest daily minimum temperature was approximately two to three times greater than the change in the highest daily maximum temperature. This implies that climate warming in the Henan Province has occurred diurnally and asymmetrically over the last 43 years, mainly because the daily maximum temperature occurs in the daytime and the daily minimum temperature occurs at night. On a seasonal scale, the highest daily maximum temperature varied most in spring followed by summer and autumn, while the smallest was in winter, with variation rates of 0.7 °C/10 a, 0.3 °C/10 a, 0.2 °C/10 a, and 0 °C/10 a, respectively. The lowest daily minimum temperature also varied most in spring; however, this was followed by winter, with the smallest in summer and autumn, with variation rates of 1.2 °C/10 a, 0.9 °C/10 a, 0.9 °C/10 a, and 1.0 °C/10 a, respectively.

**Table 3.** Variation trends of extreme temperature and extreme precipitation in Henan Province from 1978–2021 under different time scales. The \* represents passing the 0.05 significance test.

Treatments	Extreme Temperature		Extreme Precipitation
	The Maximum Value of Daily Maximum Temperature	The Minimum Value of Daily Minimum Temperature	
Spring	0.07 *	0.12 *	−0.12
Summer	0.03 *	0.09 *	1.69
Autumn	0.02 *	0.09 *	−0.19
Winter	0	0.1 *	0.15 *
Year	0.03 *	0.1 *	1.69

Due to asymmetric warming (Table 3), the daily temperature range in the Henan Province decreased in all four seasons from 1978–2021, with variation rates of  $-0.2\text{ }^{\circ}\text{C}/10\text{ a}$ ,  $-0.4\text{ }^{\circ}\text{C}/10\text{ a}$ ,  $-0.5\text{ }^{\circ}\text{C}/10\text{ a}$ , and  $-0.5\text{ }^{\circ}\text{C}/10\text{ a}$ , during spring, summer, autumn, and winter, respectively (Figure 6a–d). This phenomenon may be related to the fact that clouds are generally at lower altitudes during the day [45]. The two means by which ground temperature can increase are short-wave radiation reaching the ground through the clouds and blocking the emission of long-wave radiation from the ground. The higher cloud cover and the decrease in the low- and medium-altitude cloud cover at noon implies that the ground received more solar short-wave radiation during this time, resulting in a higher temperature. Of note, the largest decrease in the daily temperature range was obtained in summer and autumn, implying that heat wave events are more intense during these seasons.

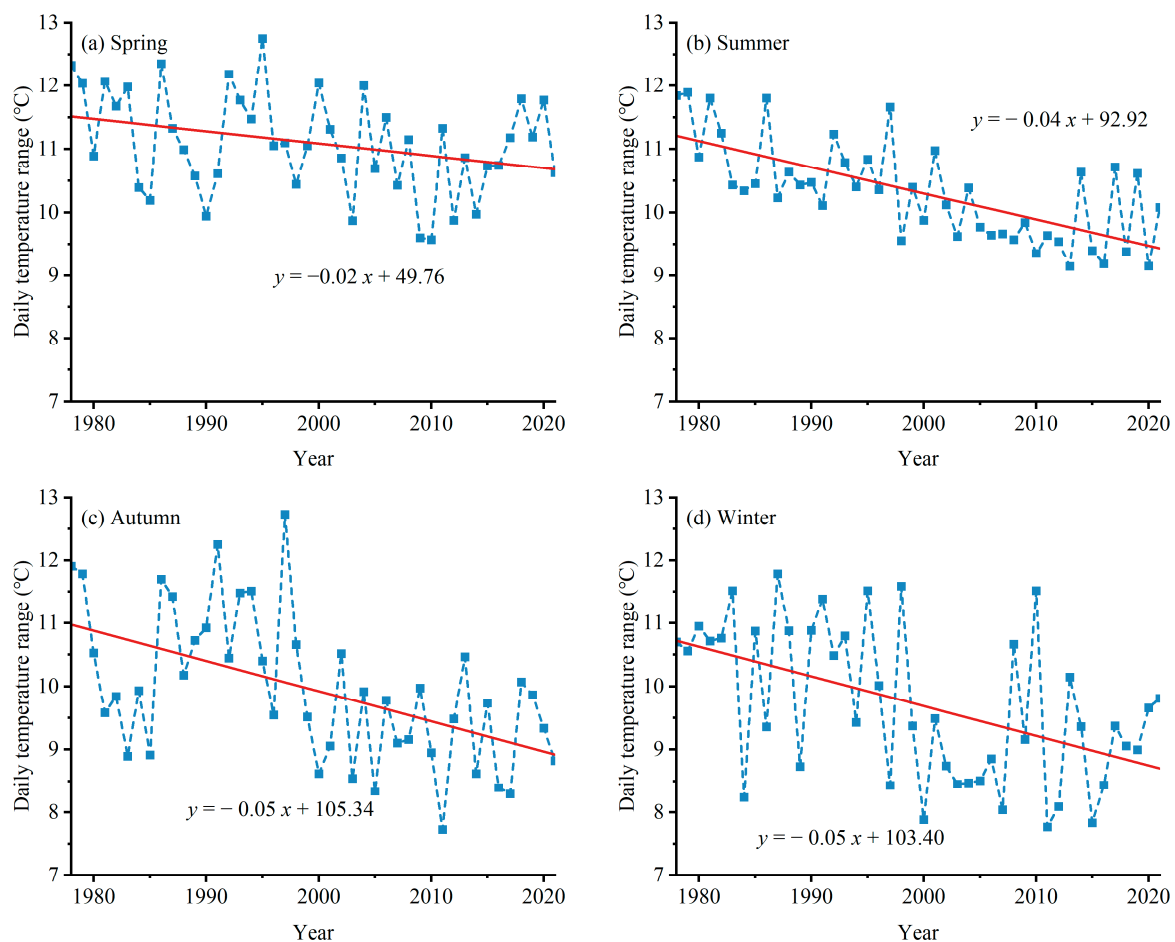


**Figure 6.** Variation trends of the daily temperature range in Henan Province from 1978–2021 under seasonal scale. (a–d) represent the seasonal scale, where (a) represents spring, (b) represents summer, (c) represents autumn, and (d) represents winter.

A non-significant increasing trend was observed for extreme precipitation on an annual scale, with variation rate of  $16.9\text{ mm}/10\text{ a}$  (Table 3). On a seasonal scale, extreme precipitation showed a non-significant decrease in spring and autumn, a non-significant increase in summer, and a significant increase in winter, with variation rates of  $-1.2\text{ mm}/10\text{ a}$ ,  $-1.9\text{ mm}/10\text{ a}$ ,  $16.9\text{ mm}/10\text{ a}$ , and  $1.5\text{ mm}/10\text{ a}$ , respectively (Table 3). These results demonstrated an increase in the intensity of extreme precipitation events in summer.

### 3.4. Variation Characteristics in the Grain Yield from 1978–2021

The grain yield in the Henan Province increased with high fluctuation over the 1978–2021 period, during which it increased by 192.40 kg/(hm<sup>2</sup>·a) with an average yield of 8801.95 kg/hm<sup>2</sup>. The climate yield fluctuated widely during this period, over the range of −1838.12 to 797.49 kg/hm<sup>2</sup> (Figure 7a). The peaks and valleys for grain yield were consistent with those of the climate yield, indicating that climate change was responsible for the fluctuations. For example, in the autumn of 2003, the increase in the number of low temperature and precipitation days meant that the accumulated temperature was below average during the crop growth period, and the severely flooded fields led to an autumn grain yield of only 3062 kg/hm<sup>2</sup> (Figure 7b).

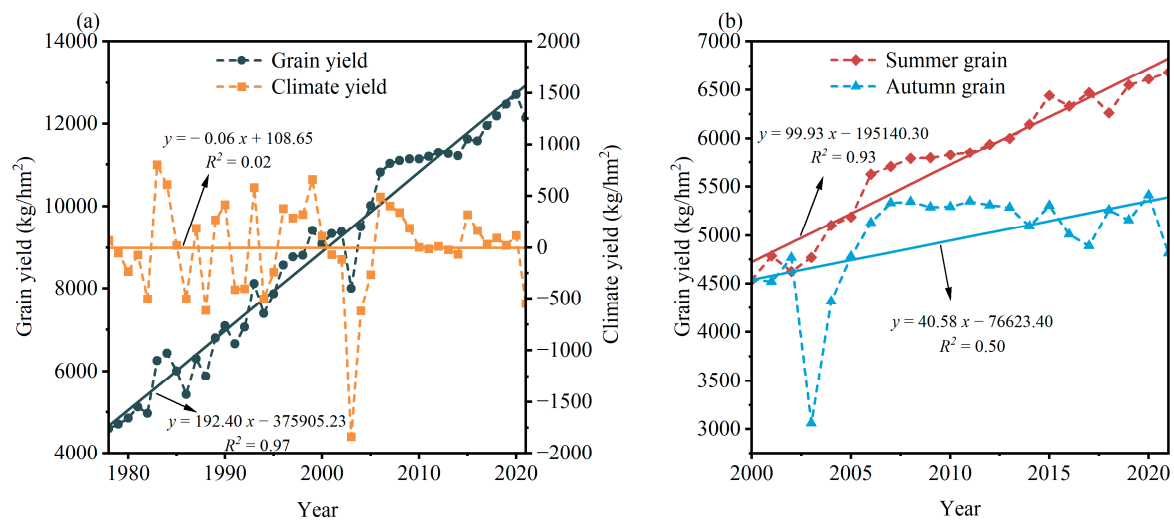


**Figure 7.** Variation characteristics of grain yield in Henan Province. (a) represents the variation characteristics of grain yield and climate yield from 1978–2021, (b) represents the variation characteristics of summer and autumn grain yields from 2000–2021.

The average summer and autumn grain yields of 5574.68 kg/hm<sup>2</sup> and 4967.21 kg/hm<sup>2</sup> for the Henan Province from 2000–2021, respectively, showed an increasing trend of 99.93 kg/(hm<sup>2</sup>·a) and 40.58 kg/(hm<sup>2</sup>·a), respectively, which fluctuated significantly and was greater in the summer than in the autumn (Figure 7b). The fluctuation in the autumn grain yield was also greater than that in summer. These results suggest that climate change has the highest impact on grain production during autumn in the Henan Province.

### 3.5. Correlation Analysis

The correlation between grain yield and water and thermal elements indicators in the Henan Province under different time scales are presented in Table 4. On an annual scale, the grain yield in the Henan Province was more correlated with  $\geq 0$  °C accumulated temperature,  $\geq 10$  °C accumulated temperature, and precipitation (the correlation degree ranged from 0.606–0.636), followed by daily temperature range and extreme precipitation (with correlation ranging from 0.475–0.577). Climate yield was equally correlated with all indicators. On the seasonal scale, the summer grain yield in the Henan Province was most correlated with the daily temperature range (correlation degree of 0.976), followed by  $\geq 0$  °C accumulated temperature,  $\geq 10$  °C accumulated temperature, and precipitation (correlation degree of 0.901–0.924), and least correlated with extreme precipitation (correlation degree of 0.588); autumn grain yield was most correlated with  $\geq 0$  °C accumulated temperature,  $\geq 10$  °C accumulated temperature, and daily temperature range (correlation degree of 0.946–0.964), followed by precipitation (correlation degree of 0.926), and least correlated with extreme precipitation (correlation degree of 0.901). Evidently, the grain yield in the

Henan Province is most correlated with temperature followed by precipitation and extreme precipitation at the different time scales.

**Table 4.** The correlation degree between grain yield and indicators of water and thermal elements in Henan Province under different time scales.

Time Scale	Yield Type	$\geq 0\text{ }^{\circ}\text{C}$ Accumulated Temperature	$\geq 10\text{ }^{\circ}\text{C}$ Accumulated Temperature	Precipitation	Daily Temperature Range	Extreme Precipitation
Year	Grain yield	0.606	0.611	0.636	0.577	0.475
	Climate yield	0.786	0.786	0.788	0.787	0.779
Spring-autumn- winter	Summer grain yield	0.924	0.901	0.911	0.976	0.588
Summer	Autumn grain yield	0.959	0.964	0.926	0.946	0.901

## 4. Discussion

### 4.1. Variation Characteristics of Water and Thermal Elements

In the present study, we found an increasing trend for both the  $\geq 0\text{ }^{\circ}\text{C}$  and  $\geq 10\text{ }^{\circ}\text{C}$  accumulated temperatures and precipitation on both the annual and seasonal scales (except for spring). Overall, the climate in the Henan Province is expected to become “warmer and wetter” in the future, while spring will be “warmer and drier”. The results of this study were similar to those reported by Tao et al. [46] and Xiao et al. [47], who predicted an increase in both temperature and precipitation on the North China Plain from 2041–2070, implying that the water supply pressure on crop production might be relieved later in the Henan Province. Hu et al. [21] investigated the distribution and variation characteristics of the agricultural thermal resources in China from 1961–2010, with results showing increases in the  $\geq 0\text{ }^{\circ}\text{C}$  and  $\geq 10\text{ }^{\circ}\text{C}$  accumulated temperatures of  $69.6\text{ }^{\circ}\text{C}/10\text{ a}$  and  $71.1\text{ }^{\circ}\text{C}/10\text{ a}$ , respectively. The  $\geq 10\text{ }^{\circ}\text{C}$  accumulated temperature in the Henan Province showed a decreasing trend in the 1960s and 1980s, followed by an increasing trend during the 1970s, 1990s, and in the 2000–2009 period [48]. The increasing rate of accumulated temperature obtained in this study was larger than that obtained in a previous study, probably because of the different periods studied. Moreover, the worsening warming trend implies that the increase in accumulated temperature will be greater because of the later start and end of the study period. A non-significant decrease in precipitation that was previously observed in North China from 1961–2014 differed from the present results [20]. This is likely because the studies are concentrated on different regions in China.

Although climate change has enriched the water and thermal resources in the Henan Province, the intensity of extreme temperature and precipitation increased. In this study, we noticed that the warming trend in the Henan Province was greater at night than during the day. Moreover, the increase in the daily minimum temperature was approximately two to three times higher than that of the daily maximum temperature. Tan et al. [49] pointed out that increases in the surface land temperature have been significantly faster at night over the past 50 years globally, with the warming rate 1.4 times higher at night than during the day. The diurnal asymmetric warming observed in this study was consistent with the findings of Tan et al. [49]; however, the warming rate obtained in this study was considerably greater.

### 4.2. Effect of Climate Change on Grain Yield

Climate change is associated with both opportunities and challenges for agricultural production in the Henan Province. The increase in the accumulated temperature and precipitation provides more water and thermal resources for crops, which is beneficial for late maturing crops and enriching the layout diversity within the region [50]. However, the increase in accumulated temperature has shortened the crop growth period, reducing the amount of time available for crop photosynthesis and decreasing biomass accumulation,

which will eventually reduce crop yields [51]. Furthermore, climate warming has heightened extreme climate events and agricultural disasters, with problems such as heat waves, droughts, floods, plant diseases, and insect pests negatively impacting grain yield [52,53]. Rosenzweig et al. [54] noted that increased temperatures improved agricultural productivity at high altitudes and limited agricultural productivity at low and medium altitudes [55]. Climate change, therefore, has both positive and negative impacts on grain yield; however, the negative impact on grain yield is more significant in most regions [56].

In this study, we found that climate change caused fluctuating changes in the grain yield of the Henan Province, hindering growth to some extent (Figure 6). We also found that grain yield was not reduced in years with lower precipitation, while reductions were observed in years with higher precipitation (Figure 7a,b). For example, despite the different degrees of drought in the spring, summer, and autumn of 2013, the grain yield in Henan Province did not decrease, with a grain yield of 11262.14 kg/hm<sup>2</sup>, while the autumn grain yield in 2021 decreased because of an extreme precipitation event in the central and northern parts of Henan from 17–22 July. Extreme weather events reduce agricultural production efficiency [57]. The results revealed that the relevant agricultural departments and farmers can take appropriate management measures to mitigate against agricultural drought but lack the appropriate management measures and treatment plans in response to extreme precipitation and secondary flooding.

Our study investigated how water and thermal resources are changing grain yields in Henan Province, China, because of climate change. Despite the significant correlations between climate change and grain yields, our study did not explain the impact of climate factors on crop water consumption during the growth period of winter wheat-summer maize, nor did it predict future changes in crop yield. Crop modeling driven by projected future climate data is a useful tool to study the likely impacts of climate change on crop yield [58]. Therefore, we recommend that further studies should use crop modeling to analyze the impact of climate change on crop yield and crop water consumption in Henan Province.

#### 4.3. Measures to Respond to Climate Change

To respond to the impact of climate change on grain yield, it is necessary to explore and develop coping strategies with adaptation or mitigation characteristics. Hardelin et al. [59] proposed a method that could improve the resilience of agriculture to climate change in three ways: strengthening the adaptive capacity of agriculture, establishing beneficial environmental conditions, and utilizing technological tools. In the future, we should respond to climate change by improving resource utilization through sustainable production intensification, improving water management measures, and enhancing the resilience of small-scale farmers to climate change by using biotechnological innovations such as crop varieties that can tolerate high temperatures, droughts and floods, plant diseases, and pests [55,60,61].

## 5. Conclusions

In this study, the trends of water and thermal resources change and their impacts on grain yield were evaluated for Henan Province on multiple time scales. The trends in water and thermal resources change were analyzed using the least squares method, Mann-Kendall method, and wavelet analysis method, respectively, and their impacts on grain yield were evaluated using the gray correlation analysis method. The major results can be concluded as follows:

(1) The climate in the Henan Province has become “warmer and wetter” over the last 43 years on an annual scale, while it is “warmer and drier” in spring and “warmer and wetter” in summer, autumn, and winter on a seasonal scale.

(2) The temperature in Henan Province has shown a diurnal asymmetric warming over the last 43 years. The increase in the lowest daily minimum temperature was approximately two to three times greater than the change in the highest daily maximum temperature.

Extreme precipitation in Henan Province has exhibited a non-significant increasing trend over the last 43 years at the annual scale. On a seasonal scale, the intensity of extreme precipitation events has increased during the summer.

(3) Climate change caused fluctuations in the grain yield of the Henan Province. Moreover, the impact of climate change on the grain yield of the Henan Province had a time scale effect. Summer and autumn grain yields showed a fluctuating upward trend from 2000–2021, while the autumn grain yield fluctuated more than the summer grain yield. These results emphasize the need to focus on the impact of climate change during autumn in the future.

(4) The grain yield in Henan Province was most correlated with temperature, followed by precipitation and extreme precipitation at different time scales.

**Author Contributions:** Conceptualization, X.F., F.W. and S.Z.; methodology, X.F., F.W., S.Z. and D.W.; software, X.F., Y.Z. and Q.C.; validation, X.F. and S.Z.; formal analysis and investigation, X.F., F.W., S.Z. and D.W.; resources, S.Z. and F.W.; data curation and writing—original draft, X.F., F.W., S.Z. and D.W.; writing—review and editing, X.F., F.W., S.Z. and D.W.; visualization, X.F., Y.Z. and Q.C.; supervision, F.W. and S.Z.; project administration, F.W. and S.Z.; funding acquisition, F.W. and S.Z.. All authors have read and agreed to the published version of the manuscript.

**Funding:** This research was supported by the National Natural Science Foundation of China (51979108), National Key Research and Development Program of China (2022YFD1900402), the Zhongyuan Science and Technology Innovation Leadership Project (194200510008), National Key Research and Development Program of China (2016YFC0400103) and the Innovation Funds of NCWU for Doctoral Candidate (B2020081505).

**Institutional Review Board Statement:** Not applicable.

**Informed Consent Statement:** Not applicable.

**Data Availability Statement:** Data recorded in the current study are available in all tables and figures of the manuscript.

**Acknowledgments:** We would like to thank the editor and the expert reviewers for their detailed comments and suggestion for the manuscript. These were very useful to hopefully improve the quality of the manuscript.

**Conflicts of Interest:** The authors declare no conflict of interest.

## References

1. IIPCC. *Climate Change 2021: The Physical Science Basis. Contribution of Working Group I to the Sixth Assessment Report of the Intergovernmental Panel on Climate Change*; Masson-Delmotte, V., Zhai, P., Pirani, A., Connors, S., Péan, C., Berger, S., Caud, N., Chen, Y., Goldfarb, L., Gomis, M., et al., Eds.; Cambridge University Press: Cambridge, UK; New York, NY, USA, 2021.
2. IPCC. *Climate Change and Land: An IPCC Special Report on Climate Change, Desertification, Land Degradation, Sustainable Land Management, Food Security, and Greenhouse Gas Fluxes in Terrestrial Ecosystems*; Shukla, P., Skea, J., Buendia, E.C., Masson-Delmotte, V., Pörtner, H.-O., Roberts, D.C., Zhai, P., Slade, R., Connors, S., van Diemen, R., et al., Eds.; Cambridge University Press: Cambridge, UK, 2019.
3. Chen, T.; Bao, A.; Jiapaer, G.; Guo, H.; Zheng, G.; Jiang, L.; Chang, C.; Tuerhanjiang, L. Disentangling the relative impacts of climate change and human activities on arid and semiarid grasslands in Central Asia during 1982–2015. *Sci. Total Environ.* **2019**, *653*, 1311–1325. [[CrossRef](#)] [[PubMed](#)]
4. Sui, Y.; Lang, X. Projected signals in climate extremes over China associated with a 2 °C global warming under two RCP scenarios. *Int. J. Climatol.* **2018**, *38*, e678–e697. [[CrossRef](#)]
5. Huang, J.; Yu, H.; Han, D.; Zhang, G.; Wei, Y.; Huang, J.; An, L.; Liu, X.; Ren, Y. Declines in global ecological security under climate change. *Ecol. Indic.* **2020**, *117*, 106651. [[CrossRef](#)]
6. Gay, C.; Estrada, F.; Conde, C.; Eakin, H.; Villers, L. Potential impacts of climate change on agriculture: A case of study of coffee production in Veracruz, Mexico. *Clim. Chang.* **2006**, *79*, 259–288. [[CrossRef](#)]
7. Kumilachew, Y.; Hatiye, S. The dual impact of climate change on irrigation water demand and reservoir performance: A case study of Koga irrigation scheme, Ethiopia. *Sustain. Water Resour. Manag.* **2022**, *8*, 25. [[CrossRef](#)]
8. Rudolf, R. The impact of maize price shocks on household food security: Panel evidence from Tanzania. *Food Policy* **2019**, *85*, 40–54. [[CrossRef](#)]
9. Xu, D.; Li, Y.; Gong, S.; Zhang, B. Impacts of climate change on agricultural water management and its coping strategies. *Trans. Chin. Soc. Agric. Eng.* **2019**, *35*, 79–89.

10. FAO; IFAD; UNICEF; WHO. Transforming Food Systems for Affordable Healthy Diets. In *The State of Food Security and Nutrition in the World 2021*; Food and Agriculture Organization of the United Nations: Rome, Italy, 2021.
11. Dong, B.; Hu, Q.; Pan, X.; He, Q.; Jiang, H.; Qiao, Y.; Wang, X.; Wei, P.; Zhao, H.; Zhang, X. Spatiotemporal distribution and variation of heat resources in the Twenty-Four Solar Terms in North China Plain over the period 1961–2014. *Chin. J. Agrometeorol.* **2017**, *38*, 131–140.
12. Hao, C.; Li, M. Spatio-temporal characters of  $\geq 0$  °C and  $\geq 10$  °C accumulated temperatures from 1960 to 2009 in Henan Province. *Chin. J. Agric. Resour. Reg. Plan.* **2019**, *40*, 89–95.
13. He, W.; Bu, R.; Xiong, Z.; Hu, Y. Characteristics of temperature and precipitation in Northeastern China from 1961 to 2005. *Acta Ecol. Sin.* **2013**, *33*, 519–531. [[CrossRef](#)]
14. Wang, F.; Liu, H.; Wu, D.; Wang, C.; Yao, S. Variation of effective accumulated temperature for winter wheat in North China Plain over the Past 30 years. *Meteorol. Environ. Sci.* **2017**, *40*, 20–27. [[CrossRef](#)]
15. Zhang, Y.; Wu, B.; Guo, B. Characteristics of agro-meteorological climate resource during maize growing season under global climate change in Sichuan Province. *Southwest China J. Agric. Sci.* **2020**, *33*, 2102–2111. [[CrossRef](#)]
16. Yu, Z.; Fan, G.; Hua, W.; Zhou, D.; Lai, X.; Liu, Y. Variation characteristics of season start dates over China under the global warming. *Clim. Environ. Res.* **2010**, *15*, 73–82.
17. Huang, J.; Zhang, G.; Yu, H.; Wang, S.; Guan, X.; Ren, Y. Characteristics of climate change in the Yellow River basin during recent 40 years. *J. Hydraul. Eng.* **2020**, *51*, 1048–1058. [[CrossRef](#)]
18. Lin, H.; Wang, J.; Huang, J.; Jiang, C. Climate drought in Huai River Basin under climate change. *China Rural. Water Hydropower* **2020**, *6*, 21–26+35.
19. Dong, G.; Li, L.; Zheng, G. Changing trends of winter temperature in recent 53 years in Ningxia and impact for agriculture. *Adv. Earth Sci.* **2016**, *31*, 1172–1181.
20. Hu, Q.; Dong, B.; Pan, X.; Jiang, H.; Pan, Z.; Qiao, Y.; Shao, C.; Ding, M.; Yin, Z.; Hu, L. Spatiotemporal variation and causes analysis of dry-wet climate over period of 1961–2014 in China. *Trans. Chin. Soc. Agric. Eng.* **2017**, *33*, 124–132+315.
21. Hu, Q.; Pan, X.-B.; Shao, C.; Zhang, D.; Wang, X.; Wei, X. Distribution and variation of China agricultural heat resources in 1961–2010. *Chin. J. Agrometeorol.* **2014**, *35*, 119–127.
22. Ren, G.; Ren, Y.; Zhan, Y.; Sun, X.; Liu, Y.; Chen, Y.; Wang, T. Spatial and temporal patterns of precipitation variability over mainland China: II Recent trends. *Adv. Water Sci.* **2015**, *26*, 451–465. [[CrossRef](#)]
23. Duan, J.; Yuan, J.; Xu, X.; Ju, H. Interpretation of the IPCC AR6 report on agricultural systems. *Clim. Chang. Res.* **2022**, *18*, 422–432.
24. Tao, F.; Zhang, Z.; Zhang, S.; Rötter, R.P.; Shi, W.; Xiao, D.; Liu, Y.; Wang, M.; Liu, F.; Zhang, H. Historical data provide new insights into response and adaptation of maize production systems to climate change/variability in China. *Field Crops Res.* **2016**, *185*, 1–11. [[CrossRef](#)]
25. Zhang, Y.; Niu, H.; Yu, Q. Impacts of climate change and increasing carbon dioxide levels on yield changes of major crops in suitable planting areas in China by the 2050s. *Ecol. Indic.* **2021**, *125*, 107588. [[CrossRef](#)]
26. Shaffril, H.; Krauss, S.; Samsuddin, S.F. A systematic review on Asian’s farmers’ adaptation practices towards climate change. *Sci. Total Environ.* **2018**, *644*, 683–695. [[CrossRef](#)] [[PubMed](#)]
27. Zhao, R.; Wang, H.; Dong, Y. Impact of climate change on grain yield and its trend across Guanzhong region. *Chin. J. Eco-Agric.* **2020**, *28*, 467–479. [[CrossRef](#)]
28. Gao, J.; Chu, B.; Yan, J.; Zhao, G. Estimation of climate production potential of corn and optimization of planting space in Henan Province from 1960. *Trans. Chin. Soc. Agric. Mach.* **2019**, *50*, 245–254.
29. Zhang, R.; Ning, X.; Qin, Y.; Zhao, K.; Li, Y. Analysis of sensitivity of main grain crops yield to climate change since 1980 in Henan Province. *Resour. Sci.* **2018**, *40*, 137–149.
30. Pang, Y.; Chen, C.; Guo, X.; Xu, F. Analysis of annual climate types and potential yield for single cropping rice in Southwest China during 1961–2015. *J. Nat. Resour.* **2021**, *36*, 476–489. [[CrossRef](#)]
31. Yang, C.; Shen, W.; Li, H. Response of grain yield in Tibet to climate and cultivated land change during 1985–2010. *Trans. Chin. Soc. Agric. Eng.* **2015**, *31*, 261–269.
32. Zai, S.; Feng, X.; Wu, F.; Li, L. Effect of time scales on probability of irrigation water requirement of farmland. *Trans. Chin. Soc. Agric. Eng.* **2018**, *34*, 96–102.
33. Lu, S.; Liu, Y.; Long, H.; Guan, X. Agricultural Production Structure Optimization: A Case Study of Major Grain Producing Areas, China. *J. Integr. Agric.* **2013**, *12*, 184–197. [[CrossRef](#)]
34. Kuang, B.; Lu, X.; Han, J.; Zhang, Z. Regional differences and dynamic evolution of cultivated land use efficiency in major grain producing areas in low carbon perspective. *Nongye Gongcheng Xuebao/Trans. Chin. Soc. Agric. Eng.* **2018**, *34*, 1–8. [[CrossRef](#)]
35. Henan Provincial Bureau of Statistics. *Henan Statistical Yearbook-2021*; China Statistics Press: Beijing, China, 2021.
36. Jiang, H. *Agricultural Meteorology*; Science Press: Beijing, China, 2008.
37. Chang, Q.; Wang, J.; Yu, W.; Zhang, N.; Li, M.; Li, W.; Huang, M. Spatiotemporal variation and potential of heat use efficiency of wheat-maize rotation system in Henan Province. *Resour. Sci.* **2019**, *41*, 1176–1187.
38. Zhou, B. Study on the Distribution and High Efficient Utilization of Resources for Double Cropping System in the Huang-Huai-Hai Plain. Ph.D. Thesis, China Agricultural University, Beijing, China, 2015.
39. Li, Y.; Zhou, M. Variation trends in water requirement of cotton and sugar beet in Xinjiang under climate change scenarios. *Trans. Chin. Soc. Agric. Eng.* **2015**, *31*, 121–128.

40. Wang, W.; Ding, J.; Li, Y. *Hydrological Wavelet Analysis*; Chemical Industry Press: Beijing, China, 2005.
41. Liu, S.; Zhang, M.; Lan, H. *Crop Yield Forecasting Methods*; Meteorological Press: Beijing, China, 1987.
42. Li, H.; Mao, L.; Mei, X.; Liu, Y.; Hao, W. Analysis on influencing factors of grain production fluctuation during the last 30 years in China. *Chin. J. Agric. Resour. Reg. Plan.* **2018**, *39*, 1–10+16.
43. Mise, E.; Kim, T.-H.; Newbold, P. On suboptimality of the Hodrick–Prescott filter at time series endpoints. *J. Macroecon.* **2005**, *27*, 53–67. [[CrossRef](#)]
44. Liu, S. *Gray System Theory and Its Applications*; Science Press: Beijing, China, 2017.
45. Wang, Y.; Bo, Y.; Wang, C. Relations of cloud amount to asymmetric diurnal temperature change in Central and Eastern Qinghai-Xizang Plateau. *Plateau Meteorol.* **2016**, *35*, 908–919.
46. Tao, F.; Zhang, Z. Adaptation of maize production to climate change in North China Plain: Quantify the relative contributions of adaptation options. *Europ. J. Agron.* **2010**, *33*, 103–116. [[CrossRef](#)]
47. Xiao, D.; Liu, D.L.; Feng, P.; Wang, B.; Waters, C.; Shen, Y.; Qi, Y.; Bai, H.; Tang, J. Future climate change impacts on grain yield and groundwater use under different cropping systems in the North China Plain. *Agric. Water Manag.* **2021**, *246*, 106685. [[CrossRef](#)]
48. Qiu, X.; Wang, J.; Zeng, Y.; Shi, G. Spatial and temporal variation characteristics of  $\geq 10^{\circ}\text{C}$  accumulated temperature and their dominant factors from 1960 to 2013 in China. *Jiangsu Agric. Sci.* **2017**, *45*, 220–225. [[CrossRef](#)]
49. Tan, J.; Piao, S.; Chen, A.; Zeng, Z.; Ciais, P.; Janssens, I.; Mao, J.; Myneni, R.; Peng, S.; Penuelas, J.; et al. Seasonally different response of photosynthetic activity to daytime and night-time warming in the Northern Hemisphere. *Glob. Chang. Biol.* **2014**, *21*, 377–387. [[CrossRef](#)]
50. Zhao, Y.; Xiao, D.; Tang, J.; Bai, H. Effects of climate change on the yield of major grain crops and its adaptation measures in China. *Reaearch Soil Water Conserv.* **2019**, *26*, 317–326. [[CrossRef](#)]
51. Asseng, S.; Martre, P.; Maiorano, A.; Rötter, R.P.; O’Leary, G.; Fitzgerald, G.; Girusse, C.; Motzo, R.; Giunta, F.; Babar, M.; et al. Climate change impact and adaptation for wheat protein. *Glob. Chang. Biol.* **2018**, *25*, 155–173. [[CrossRef](#)]
52. Holst, R.; Yu, X.; Grün, C. Climate change, risk and grain yields in China. *J. Integr. Agric.* **2013**, *12*, 1279–1291. [[CrossRef](#)]
53. Wu, J.; Zhang, J.; Ge, Z.; Xing, L.; Han, S.; Shen, C.; Kong, F. Impact of climate change on maize yield in China from 1979 to 2016. *J. Integr. Agric.* **2021**, *20*, 289–299. [[CrossRef](#)]
54. Rosenzweig, C.; Elliott, J.; Deryng, D.; Ruane, A.C.; Muller, C.; Arneth, A.; Boote, K.J.; Folberth, C.; Glotter, M.; Khabarov, N.; et al. Assessing agricultural risks of climate change in the 21st century in a global gridded crop model intercomparison. *Proc. Natl. Acad. Sci. USA* **2014**, *111*, 3268–3273. [[CrossRef](#)]
55. Wiebe, K.; Robinson, S.; Cattaneo, A. Climate change, agriculture and food security. In *Sustainable Food and Agriculture*; Elsevier: Amsterdam, The Netherlands, 2019; pp. 55–74. [[CrossRef](#)]
56. Chen, X.; Wang, L.; Niu, Z.; Zhang, M.; Li, C.a.; Li, J. The effects of projected climate change and extreme climate on maize and rice in the Yangtze River Basin, China. *Agric. For. Meteorol.* **2020**, *282–283*, 107867. [[CrossRef](#)]
57. Bai, Y.; Deng, X.; Jiang, S.; Zhao, Z.; Miao, Y. Relationship between climate change and low-carbon agricultural production: A case study in Hebei Province, China. *Ecol. Indic.* **2019**, *105*, 438–447. [[CrossRef](#)]
58. Xiao, D.; Liu, D.L.; Wang, B.; Feng, P.; Bai, H.; Tang, J. Climate change impact on yields and water use of wheat and maize in the North China Plain under future climate change scenarios. *Agric. Water Manag.* **2020**, *238*, 106238. [[CrossRef](#)]
59. Hardelin, J.; Lankoski, J. Climate change, water and agriculture: Challenges and adaptation strategies. *EuroChoices* **2015**, *14*, 10–15. [[CrossRef](#)]
60. Rasmussen, L.; Coolsaet, B.; Martin, A.; Mertz, O.; Pascual, U.; Corbera, E.; Dawson, N.; Fisher, J.; Franks, P.; Ryan, C. Social-ecological outcomes of agricultural intensification. *Nat. Sustain.* **2018**, *1*, 275–282. [[CrossRef](#)]
61. Hossain, A.; Skalicky, M.; Brestic, M.; Maitra, S.; Ashraful Alam, M.; Syed, M.A.; Hossain, J.; Sarkar, S.; Saha, S.; Bhadra, P.; et al. Consequences and Mitigation Strategies of Abiotic Stresses in Wheat (*Triticum aestivum* L.) under the Changing Climate. *Agronomy* **2021**, *11*, 241. [[CrossRef](#)]

**Disclaimer/Publisher’s Note:** The statements, opinions and data contained in all publications are solely those of the individual author(s) and contributor(s) and not of MDPI and/or the editor(s). MDPI and/or the editor(s) disclaim responsibility for any injury to people or property resulting from any ideas, methods, instructions or products referred to in the content.